

and found to be in good agreement with the predictions of a simple model based upon the small, but non-negligible, loss of spin memory during an optical cycle. This latter result shows that, in general, excitation with circularly polarized light is a necessary, although not sufficient, condition to observe the spin-dependent contribution to the

MCD signal in emission.

ACKNOWLEDGMENT

The author wishes to thank Professor D. B. Fitchen for many interesting and informative discussions.

*Work supported by the Advanced Research Projects Agency through the Materials Science Center at Cornell University, MSC Report No. 1301.

¹M. P. Fontana and D. B. Fitchen, *Phys. Rev. Letters* 23, 1497 (1969).

²For a comprehensive review of magneto-optic effects in F centers, see C. H. Henry and C. P. Slichter, in *Physics of Color Centers*, edited by W. B. Fowler (Academic, New York, 1968).

³D. Schmid and V. Zimmerman, *Phys. Letters* 27A,

459 (1968).

⁴H. Fanepucci and L. F. Mollenauer, *Phys. Rev.* 178, 589 (1969).

⁵N. V. Karlov, J. Margerie, and Y. Merle-D'Aubigne, *J. Phys. Radium*, 24, 717 (1963).

⁶L. G. Mollenauer, S. Pan, and S. Yngvesson, *Phys. Rev. Letters* 23, 683 (1966).

⁷J. A. Davis, thesis, Cornell University, 1969 (unpublished).

PHYSICAL REVIEW B

VOLUME 2, NUMBER 4

15 AUGUST 1970

M Centers in MgF₂ Crystals[†]

O. E. Facey and W. A. Sibley

Solid State Division, Oak Ridge National Laboratory, Oak Ridge, Tennessee 37830

(Received 9 March 1970)

A study of the optical absorption and emission of the *M*(C_{2h}) center in MgF₂ has been made. It is shown that excitation of the 370-nm absorption band due to these centers gives rise to polarized emission bands at 420 and 861 nm. Narrow-line transitions are observed both on the low-energy side of the 370-nm absorption band and the high-energy side of the 420-nm emission band. These lines have almost a mirror symmetry about the zero-phonon line which occurs at 387.3 nm and are attributed to transitions involving the lattice vibration modes of the crystal.

INTRODUCTION

In the cassiterite structure of MgF₂, there are four different *M*-center configurations each with its own symmetry. In this paper, we will differentiate between these configurations by designating the symmetry of the center in parentheses immediately after the *M* notation, i.e., *M*(C_{2v}), *M*(D_{2h}), *M*(C_{2h}), and *M*(C₁). Figure 1 illustrates the location of these various centers in the MgF₂ lattice. Little work has been done on either *M*(C_{2v}) or *M*(D_{2h}) centers,¹ but it has been established¹⁻³ that *M*(C_{2h}) centers absorb light of 370 nm (3.35 eV) and emit light of 420 nm (2.96 eV). The absorption band due to these centers also shows fine structure on the low-energy side that has been attributed to transitions associated with lattice phonons. The *M*(C₁) center absorbs light of 400

nm (3.10 eV) and has an emission peak at 600 nm

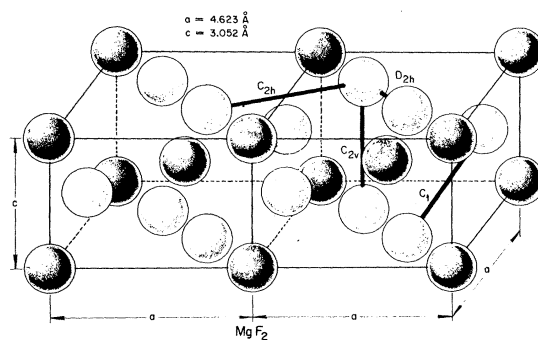


FIG. 1. MgF₂ lattice. The four possible *M*-center configurations are shown by the solid lines.

(2.07 eV).³

The purpose of this paper is to present a detailed experimental study of both the broad-band and narrow-line absorption and emission due to $M(C_{2h})$ centers. The evaluation of these data in terms of a semiclassical configuration coordinate model⁴⁻⁶ yields some insight into the validity and limitations of this model.

PROCEDURE

Single-crystal ingots of MgF_2 were purchased from the Harshaw Chemical Co. and cut into oriented optical specimens with thicknesses ranging from 0.5 to 2.0 mm. Samples were cut so that the optical faces were either perpendicular (c_1) or parallel (c_{\parallel}) to the c axis. The crystals were irradiated with 2.0-MeV electrons or ^{60}Co γ rays. Optical-absorption measurements were made using a Cary 14R spectrophotometer with a pair of Polaroid ultraviolet-type HNP'B unsupported polarizers in both the sample and reference beams. Luminescence data were taken with either an EMI 9558Q or an RCA 7102 multiplier phototube mounted to a 1-m Jarrell-Ash monochromator. Both tubes were cooled to dry-ice temperature to reduce dark current. The detection system was calibrated using a standard quartz-iodine lamp with calibration traceable to the National Bureau of Standards.⁷ A mercury lamp mounted to a $\frac{1}{2}$ -m Bausch and Lomb monochromator was used to excite the emission. Both optical-absorption and emission measurements were made with the crystals mounted in a cryostat. Specimen temperatures were measured using a Pt-resistance thermometer. When liquid helium was the refrigerant, the sample temperature was measured to be 7 °K; however, Pt-resistance thermometers are not very accurate below about 10 °K and our accuracy is about ± 2 °K. More complete details of the crystal purity and experimental techniques have been given previously.³

EXPERIMENTAL RESULTS

The normalized absorption and luminescence at 6 °K from $M(C_{2h})$ centers are portrayed in Fig. 2. The emission is shown on the right-hand side of the figure with the peak at 2.96 eV; and, in addition to the fine structure shown on the low-energy side of the absorption band, there is fine structure on the high-energy side of the emission band. The intensity of these lines is very weak, and their position is indicated on an expanded scale in the inset. Within the accuracy of our wavelength calibration for the Cary 14R and the Jarrell-Ash monochromator the zero-phonon lines for absorption and emission appear to occur at the same wavelength. Table I indicates the energy difference in wave numbers between the zero-phonon line in absorption and emission and the other sharp lines. The question mark shown beside the emission peak labeled 393.5 nm in the table means that our data are not very accurate for this peak, and the real peak position could be as much as 20-30 cm^{-1} different from that shown. The width at half-maximum for the absorption band is $W(7 \text{ }^{\circ}\text{K}) = 0.186 \text{ eV}$, and for the emission band it is $W(7 \text{ }^{\circ}\text{K}) = 0.216 \text{ eV}$.

Crystals that have been irradiated with only a small dose of neutrons possess emission characteristics that are essentially indistinguishable from those of samples γ or electron irradiated. In Fig. 3, the luminescence at 7 °K from a neutron-irradiated specimen is plotted versus photon energy over the range 1.0-3.5 eV for light excitation of 365 and 312 nm. Solid curves show data taken when the analyzer transmitted only light emitted with the electric vector perpendicular to the c axis of the crystal ($\vec{E}_{\perp c}$), and the dashed line portrays data for the electric vector of the emitted light parallel to the c axis ($\vec{E}_{\parallel c}$). When 365-nm exciting light is used, as in the upper panel, one unpolarized and two polarized luminescence bands can be observed. The unpolarized emission at

TABLE I. Narrow-line transitions in MgF_2 .

Absorption			Luminescence			Lattice mode	
Peak position	Energy difference		Peak position	Energy difference		Assignment	
(nm)	(cm^{-1})	(cm^{-1})	(nm)	(cm^{-1})	(cm^{-1})	(cm^{-1})	
387.3	258 20		387.0	258 46			
385.7	259 27	107	388.5	257 38	108	92 (Γ_5) or 119 (X_2)	
384.5	260 07	187	390.2	256 33	213	180 (Γ_6), 209 (X_1), or 186 (Z_2)	
382.7	261 30	310	392.0	255 20	326	298 (Γ_{10}), 325 (Γ_3), or 297 (X_3)	
380.8	262 61	441	(?) 393.5	254 23	423	438 (Γ_4), 451 (X_1), 441 (X_2)	
						446 (Z_2), or 450 (Γ_6)	

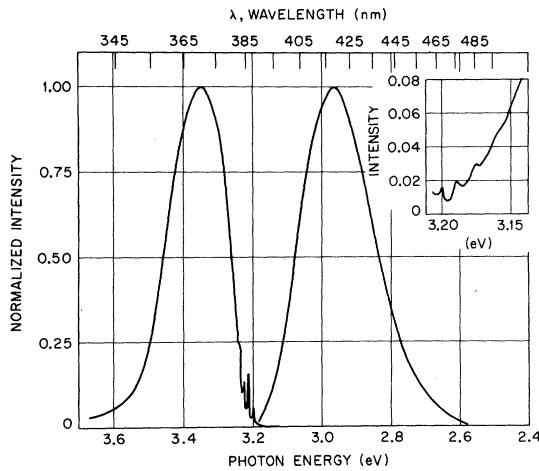


FIG. 2. Normalized absorption and emission at 7 °K of the $M(C_{2h})$ center. The sharp line structure is evident for absorption, but is so weak in the case of the luminescence that it is shown in the inset with the scale expanded.

about 600 nm is due to $M(C_1)$ centers which give rise to an absorption band at 400 nm. This band is broad enough to have appreciable absorption in the 365-nm region. The low-energy emission band shown in the top panel which peaks at 861 nm (1.44 eV) is oppositely polarized to that at 420 nm (2.96 eV) and could be a transition from the same

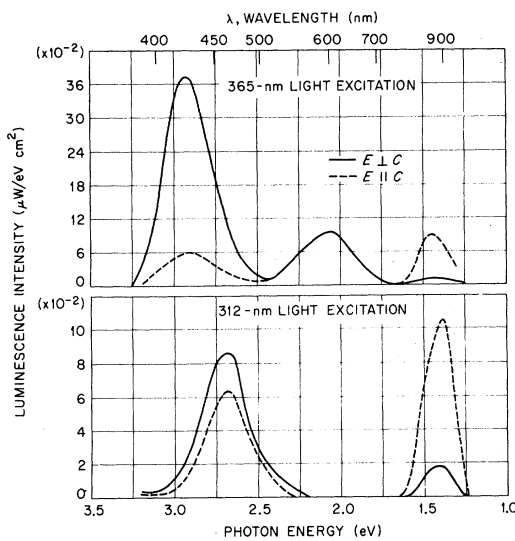


FIG. 3. Emission from neutron-irradiated MgF_2 excited by either 365- or 312-nm light. The solid line depicts data for the electric vector of the emitted light perpendicular to the c axis of the crystal. The dashed line shows data for the electric vector of the emitted light parallel to the crystalline c axis.

center responsible for this latter band. In order to see if this is the case, measurements of the intensity of both emission bands were made as a function of $M(C_{2h})$ center concentration. The results are displayed in Fig. 4. The straight-line relationship suggests that these two bands are different transitions from the same center. The two points shown below the line were obtained after the sample had been at room temperature for some time and then recooled for measurement. We do not consider these data to be as accurate as the others.

The lower panel of Fig. 3, which illustrates the emission stimulated by 312-nm light, shows two polarized emission bands at 463 nm (2.68 eV) and 900 nm (1.39 eV). Perhaps these are the π and σ transitions of the $M(D_{2h})$ centers.¹

DISCUSSION

"Vibronic" Transitions

For our purposes the concepts of the zero-phonon line and the other electron-phonon interactions of a defect are most simply discussed in terms of a configuration coordinate model such as that sketched by Hughes⁸ and by Fitchen.⁹ Within the Condon and Born-Oppenheimer approximations, the probability of an electric-dipole transition between states is proportional to the square of the matrix element connecting these states and can be written

$$P = \{ \langle \psi_e | r | \psi_g \rangle \langle \chi_m | \chi_n \rangle \}^2, \quad (1)$$

where ψ_g and ψ_e are the electron wave functions and χ_n and χ_m are the nuclear wave functions in the ground and excited states, respectively. The factor $\langle \psi_e | r | \psi_g \rangle$ is proportional to the oscillator strength of the transition and thus the transition probability is determined by the overlap integral of χ_m and χ_n . The integral has been evaluated by several different workers for the important case where $T = 0$ °K and the frequency ν of the ions is the same in the ground and excited states (the linear coupling approximation).^{6,8-10} Under these approximations the normalized transition probability is

$$P_{0m} = (S^m / m!) e^{-S}, \quad (2)$$

where S , the so-called Huang-Rhys factor, is a measure of the number of phonons given off when the defect goes from the excited to the relaxed state. If E_{00} is the energy difference between the lowest ground and excited states, then Eq. (2) leads to an absorption spectrum consisting of a series of lines at

$$E_m = E_{00} + m \hbar \nu_e. \quad (3)$$

When emission occurs between the same pair of states, then a similar series of lines at energies

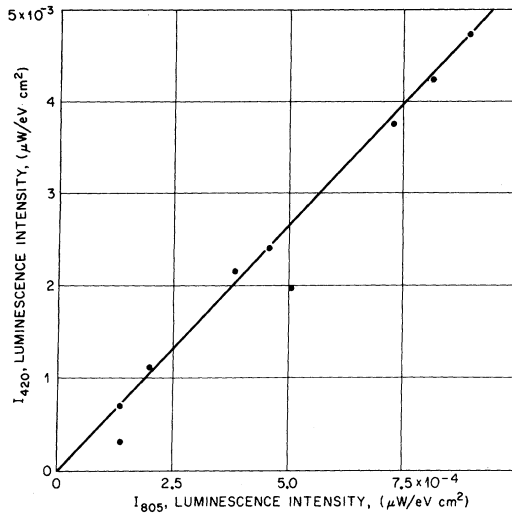


FIG. 4. Plot of the luminescence intensity at 420 nm versus the luminescence intensity at 815 nm in crystals excited by 365-nm light and containing various concentrations of $M(C_{2h})$ centers.

$$E_n = E_{00} - nh\nu_g \quad (4)$$

will appear, giving a mirror symmetry of emission and absorption about the zero-phonon line.

From the linear coupling approximation a value for S can be obtained from the expression⁶ $S_i = [W_i(0^\circ\text{K})/2.36h\nu_i]^2$ and a knowledge of W_i and ν_i in the ground and excited states. Moreover, from Eq. (2) the zero-phonon transition which occurs at E_{00} has the normalized transition probability $P = e^{-S}$ and the ratio of the area of the zero-phonon line to that of the phonon-broadened main absorption band will determine S . We have compared the areas of the broad absorption and emission bands with those of the zero-phonon lines in absorption and emission and find $S_{\text{abs}} = 4.7 S_{\text{em}} = 8.0$. From the temperature dependence of the half-width of the broad absorption and emission bands $W_{\text{abs}}(6)$ and $W_{\text{em}}(6)$, and the frequencies of ground and excited states,³ we find $S_{\text{abs}} = 5.0$ and $S_{\text{em}} = 6.5$. In view of the difficulties involved in obtaining accurate areas for the zero-phonon lines, we feel the agreement between the two methods is very good. The agreement also suggests that even when the frequencies ν_e and ν_g differ by as much as 30%, as they do in our case, the linear coupling approximation is not too bad.

Table I shows the energy difference between the zero-phonon lines and the other narrow lines observed in both absorption and emission. The fact that there is almost mirror symmetry about the zero-phonon line again suggests that the linear

coupling approximation which assumes $\nu_e = \nu_g$ and $S_e = S_g$ is not too unreasonable in this case. In the last column of Table I, assignment has been made of the possible lattice modes which give rise to the observed energy spacing. It should be remembered that there is normally a selection rule in the factor $\langle \chi_m | \chi_n \rangle$ of the transition probability [Eq. (1)]. If in the ground state χ_n has A_g symmetry, then the excited state χ_m should have this same symmetry, if the transition is to be allowed. Because there is usually a displacement of the center of the coordinate system between the ground and excited states, the normal selection rule $\langle \chi_n | \chi_m \rangle$ may appear to be violated. For the transition to occur it is only necessary for the excited state χ_m to have a component of A_g symmetry when χ_m is expanded about the same origin as χ_n . In the dispersion curves of Katiyar and Krishnan,¹¹ it is possible to find modes, as shown in Table I, that have the proper energies to match those observed and that have an A_g component when the correlation from lattice symmetry to defect symmetry is made.

Let us now investigate how well our data fit into the semiclassical configuration-coordinate analysis which does not assume linear coupling. Figure 5 illustrates the diagram that is normally used for this type of analysis. The total energy of the system is plotted on the ordinate and the abscissa specifies the configuration coordinate X . The ground and excited states of the system are represented by two parabolic curves with force constants K_g and K_e . The minima of the two states are separated in energy by E_0 and in coordinate by X_0 . The parameter E_0 is related to E_{00} by the expression $E_0 = E_{00} + h\nu_e - h\nu_g$. It is assumed that the primary mode of lattice vibration influencing the defect is a "breathing" mode and that transi-

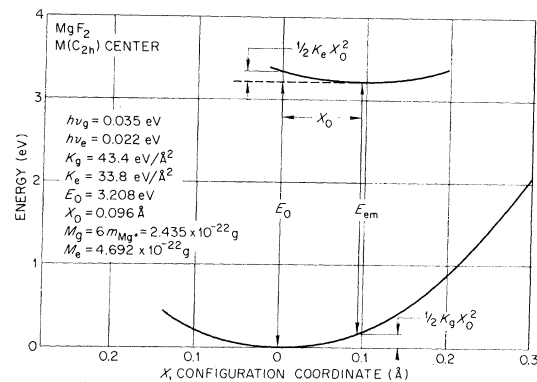


FIG. 5. Configuration-coordinate curve calculated from Eqs. (5)–(7) for the $M(C_{2h})$ center in MgF_2 .

tions between the ground and excited states are vertical. In our case at very low temperatures the absorption and emission energies can be written

$$\begin{aligned} E_{\text{abs}} &= E_0 + \frac{1}{2} K_e X_0^2 - \frac{1}{2} h\nu_g = 3.345 \text{ eV}, \\ E_{\text{em}} &= E_0 - \frac{1}{2} K_g X_0^2 + \frac{1}{2} h\nu_e = 2.963 \text{ eV}, \end{aligned} \quad (5)$$

where the numbers are taken from experimental data. Moreover, the frequencies ν_g and ν_e of the ground and excited states in terms of the force constants K_g and K_e and the mass of the vibrating system are

$$\begin{aligned} (2\pi\nu_g)^2 &= K_g/M_g, \\ (2\pi\nu_e)^2 &= K_e/M_e, \end{aligned} \quad (6)$$

where experimentally³ $\nu_g = 8.5 \times 10^{12} \text{ s}^{-1}$ and $\nu_e = 5.4 \times 10^{12} \text{ s}^{-1}$. It is customary^{4,5} to take the mass of the ground state to be the sum of the masses of the nearest neighbors so that $M_g = 6m_{\text{Mg}}$. This information, along with the expression for the half-width of the absorption and emission at low temperatures⁴

$$\begin{aligned} W_{\text{abs}} &= (4 \ln 2 h\nu_g / K_g)^{1/2} K_e X_0 = 0.186 \text{ eV}, \\ W_{\text{em}} &= (4 \ln 2 h\nu_e / K_e)^{1/2} K_g X_0 = 0.216 \text{ eV}, \end{aligned} \quad (7)$$

is sufficient to construct the configuration-coordinate diagram shown in Fig. 5. As can be seen, there seems to be good agreement between the model and experiment. Timusk¹² found that in the case of the α center in KBr it was necessary to include cubic terms in Eqs. (5) in order to fit his data. This is not necessary for the $M(C_{2h})$ center in MgF_2 since X_0 is so small.

Band Shapes

Even though we find reasonably good agreement between the simple model and the data, some difficulties remain. Lüty and Gebhardt⁴ made a similar analysis of the F center in KCl, and later Klick *et al.*⁵ pointed out that if their analysis was correct then one should be able to take their data along with the low-temperature limit for the absorption transition probability given by

$$\begin{aligned} P(E_{\text{abs}}) &= [K_e(X - \dot{X}_0)]^{-1} \\ &\times (K_g \pi h\nu_g)^{1/2} \exp(-K_g X^2 / h\nu_g), \end{aligned} \quad (8)$$

and fit the shape of the low-temperature absorption band. They found that for the F center in KCl it was possible to use the configuration-coordinate analysis to either describe the emission process or to fit the absorption band shapes over a wide range of absorption coefficients and temperature, but not to do both. One source of difficulty in the approach of Klick *et al.*⁵ is that they purposely used only absorption data to avoid such problems

as relaxation effects in the excited state and the possibility of more than one excited-state level being involved. Because of this, it was necessary to assume that the effective mass of the ground and excited states were equal. This may not be a very good assumption. In Fig. 6 we have attempted to match the shapes of the $M(C_{2h})$ absorption and emission bands with the data shown in Fig. 5; this is illustrated by the solid lines. It is evident that the agreement between theory and experiment is not very good. When we force $M_g = M_e$, as Klick *et al.* did, and yet maintain the predicted absorption and luminescence positions the same, there is even less agreement. This is illustrated by the dashed lines in Fig. 6(a). Several possible reasons for this lack of agreement exist. First, the experimental band shapes in our case are not nearly as accurate as those taken by Klick *et al.*⁵ for the F center in KCl. For example, it is not possible to determine if there is another small absorption band on the high-energy side of the $M(C_{2h})$ band which results in more absorption on this side, and there are a number of emission bands which could result in the differences shown in the inset of Fig. 6(b). Also, when the Huang-

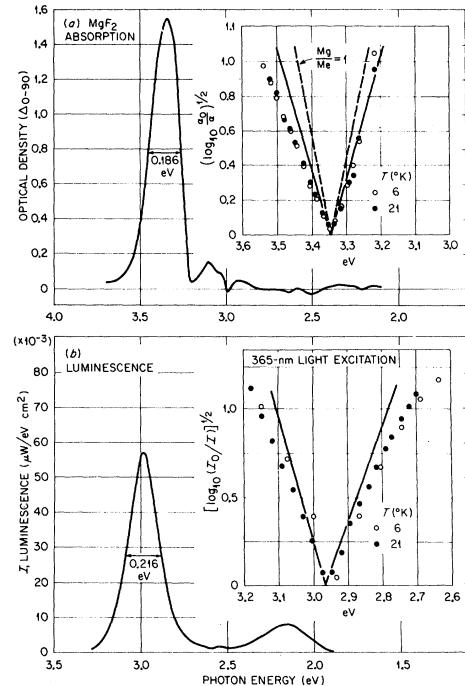


FIG. 6. Plot of the absorption and emission of the $M(C_{2h})$ center and, in the inset, the relative absorption and emission strength as a function of energy using the experimental data (points) and Eq. (8) (lines) with the data shown in Fig. 5.

Rhys factor S is small as it is here, the quantum-mechanical calculations predict a Poissonian band shape^{6,8-10} instead of Gaussian shape. This type of curve has a long tail to the violet and could be another reason for the poor fit between the data points and the solid lines drawn in Fig. 6(a).

It is evident that even in the present case with polarized bands, which should reduce baseline problems, and a zero-phonon line, which allows a good estimate of E_0 , the semiclassical configuration-coordinate analysis gives only qualitative agreement as far as band shapes are concerned. What is needed for a quantitative fit of the band shape is not only better data, but also a more complete theory.

SUMMARY

The absorption and emission of $M(C_{2h})$ centers

in MgF_2 have been studied, and it was shown that the 420- and 861-nm emission bands come from the same center. The narrow-line transitions observed both in absorption and emission have been associated with lattice modes of the crystal and appear to be what has been referred to as one-phonon transitions. Further work on the temperature dependence on these lines will allow a more accurate evaluation.

ACKNOWLEDGMENTS

The authors would like to thank R. F. Wood and B. N. Ganguly for several very helpful discussions and for their interest in this problem. J. C. Traylor has been very helpful, and we appreciate the use of his computer analysis of the vibration modes of rutile which has the same structure as MgF_2 .

¹Research sponsored by the U. S. Atomic Energy Commission, under contract with Union Carbide Corporation, Oak Ridge, Tenn.

²R. F. Blunt and M. I. Cohen, Phys. Rev. 153, 1031 (1967).

³W. A. Sibley and O. E. Facey, Phys. Rev. 174, 1076 (1968).

⁴O. E. Facey and W. A. Sibley, Phys. Rev. 186, 926 (1969).

⁵F. Lüty and W. Gebhardt, Z. Physik 169, 475 (1962).

⁶C. C. Klick, D. A. Patterson, and R. S. Knox, Phys. Rev. 133, A1717 (1964).

⁷J. J. Markham, in *Solid State Physics*, edited by F.

Seitz and D. Turnbull (Academic, New York, 1966), Suppl. 8; Rev. Mod. Phys. 31, 956 (1959).

⁸R. Stair, W. E. Schneider, and J. K. Jackson, Appl. Opt. 2, 1151 (1963).

⁹A. E. Hughes, J. Phys. (Paris), Suppl. C4, 28, 55 (1967).

¹⁰D. B. Fitchen, in *The Physics of Color Centers*, edited by W. B. Fowler (Academic, New York, 1968).

¹¹T. Keil, Phys. Rev. 140, A601 (1965).

¹²R. S. Katiyar and R. S. Krishnan, Can. J. Phys. 45, 3079 (1967).

¹³T. Timusk, J. Phys. Chem. Solids 26, 849 (1965).